

# Mott-Hubbard exciton in the optical conductivity of $\text{YTiO}_3$ and $\text{SmTiO}_3$

A. Gössling<sup>1</sup>, R. Schmitz<sup>2</sup>, H. Roth<sup>1</sup>, M.W. Haverkort<sup>1</sup>, T. Lorenz<sup>1</sup>,  
J.A. Mydosh<sup>1</sup>, E. Müller-Hartmann<sup>2</sup>, and M. Grüninger<sup>1,3</sup>

<sup>1</sup>*II. Physikalisches Institut, Universität zu Köln, Zülpicher Strasse 77, D-50937 Köln, Germany*

<sup>2</sup>*Institut für Theoretische Physik, Universität zu Köln, Zülpicher Strasse 77, D-50937 Köln, Germany*

<sup>3</sup>*2. Physikalisches Institut A, RWTH Aachen University,  
Otto-Blumenthal-Strasse, D-52074 Aachen, Germany*

(Dated: May 16, 2008)

In the Mott-Hubbard insulators  $\text{YTiO}_3$  and  $\text{SmTiO}_3$  we study optical excitations from the lower to the upper Hubbard band,  $|d^1d^1\rangle \rightarrow |d^0d^2\rangle$ . The multi-peak structure observed in the optical conductivity reflects the multiplet structure of the upper Hubbard band in a multi-orbital system. Absorption bands at 2.55 and 4.15 eV in the ferromagnet  $\text{YTiO}_3$  correspond to final states with a triplet  $d^2$  configuration, whereas a peak at 3.7 eV in the antiferromagnet  $\text{SmTiO}_3$  is attributed to a singlet  $d^2$  final state. A strongly temperature-dependent peak at 1.95 eV in  $\text{YTiO}_3$  and 1.8 eV in  $\text{SmTiO}_3$  is interpreted in terms of a Hubbard exciton, i.e., a charge-neutral (quasi-)bound state of a hole in the lower Hubbard band and a double occupancy in the upper one. The binding to such a Hubbard exciton may arise both due to Coulomb attraction between nearest-neighbor sites and due to a lowering of the kinetic energy in a system with magnetic and/or orbital correlations. Furthermore, we observe anomalies of the spectral weight in the vicinity of the magnetic ordering transitions, both in  $\text{YTiO}_3$  and  $\text{SmTiO}_3$ . In the  $G$ -type antiferromagnet  $\text{SmTiO}_3$ , the *sign* of the change of the spectral weight at  $T_N$  depends on the polarization. This demonstrates that the temperature dependence of the spectral weight is not dominated by the spin-spin correlations, but rather reflects small changes of the orbital occupation.

PACS numbers: 71.20.Be, 71.27.+a, 77.84.Dy, 78.20.-e, 78.20.Ci

## I. INTRODUCTION

In strongly correlated electron systems, the competition between kinetic energy and Coulomb repulsion gives rise to a variety of intriguing phenomena.<sup>1,2</sup> The most simple approach is the single-band Hubbard model, with on-site Coulomb repulsion  $U$  and a kinetic part proportional to the inter-site hopping amplitude  $t$ . For  $U$  larger than the band width, the band splits into a lower and an upper Hubbard band (LHB and UHB, see inset of Fig. 1). At half filling one finds a Mott-Hubbard insulator with one localized electron per site, i.e., the Coulomb energy dominates. However, the low-energy physics is determined by the kinetic energy: virtual hopping of the electrons to neighboring sites is effectively described by exchange interactions with  $J \propto t^2/U$ . These govern the spin degrees of freedom and, in a multi-orbital model, are also relevant for the orbital degrees of freedom.<sup>3,4,5</sup>

The competition between Coulomb energy and kinetic energy also governs the formation of bound states, e.g., excitons. In simple band insulators, binding of an electron in the conduction band and a hole in the valence band reduces the Coulomb energy, while the kinetic energy increases. In Mott-Hubbard insulators, the lowest optical “interband” excitation creates an empty site and a doubly occupied site, i.e., a hole in the LHB and a particle in the UHB. A Hubbard exciton can be regarded as a bound state of an empty site and a doubly occupied site, moving in a background of singly occupied sites. Studies of excitons in correlated electron systems thus far have focused on one- (1D) or two-dimensional (2D) systems. Remarkably, it has been found that ex-

citon binding can be driven by either the Coulomb energy or the kinetic energy. The former is found in the 1D extended Hubbard model, which takes into account the Coulomb interaction  $V$  between nearest or next-nearest neighbor sites.<sup>6,7,8,9,10,11,12,13,14</sup> Since *both* the Mott-Hubbard gap and the attractive interaction for exciton binding result from Coulomb interactions, one expects different physics compared to band insulators. In fact, excitons are only formed below the gap if  $V$  exceeds a critical value.<sup>6,7,9,11</sup> For smaller values of  $V$ , an excitonic resonance is found in the continuum above the gap, strongly affecting the line shape of the optical conductivity  $\sigma(\omega)$ .<sup>9,11,14</sup> An exciton below the gap has been observed in 1D Ni-halogen chains,<sup>15,16</sup> and this exciton contributes to the gigantic non-linear optical response observed in these compounds.<sup>14,15,16,17</sup>

The kinetic energy is of prime importance for excitons in the 2D cuprates,<sup>18,19,20,21,22,23,24,25,26,27,28,29</sup> which are of charge-transfer type. The dispersion of a spinless charge-transfer exciton is of order  $t$ , *larger* than the single-particle dispersion, which is suppressed to  $\sim J$  by antiferromagnetic (AF) correlations. Thus exciton formation reduces the *kinetic* energy,<sup>18,19,20,21,22</sup> which bears resemblance to a possible mechanism for Cooper pair formation in high- $T_c$  superconductors.<sup>21,30,31</sup> Experimentally, the exciton dispersion has been studied by electron-energy-loss spectroscopy<sup>19</sup> and by resonant inelastic x-ray scattering (RIXS).<sup>28,29</sup> It has been claimed that the dispersion is indeed large,<sup>19,28</sup> but recent high-resolution RIXS data<sup>29</sup> indicate that the exciton dispersion is suppressed by the coupling to phonons.

Here, we report on the observation of an excitonic res-

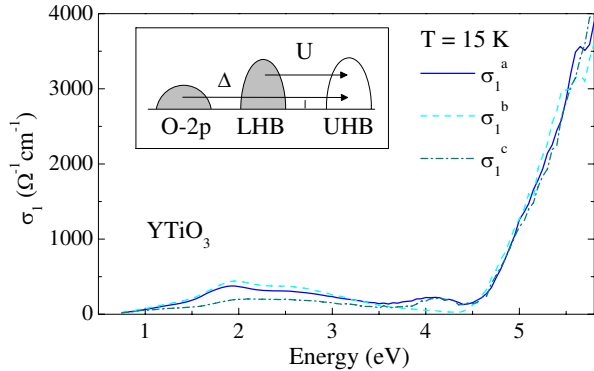


FIG. 1: (Color online) Optical conductivity of  $\text{YTiO}_3$  at 15 K. *Inset:* sketch of the optical excitations from the lower Hubbard band (LHB) and the oxygen  $2p$  band into the upper Hubbard band (UHB) in case of a single, half-filled orbital at the transition-metal site.

onance in the optical conductivity  $\sigma(\omega)$  of the 3D Mott-Hubbard insulators  $\text{YTiO}_3$  and  $\text{SmTiO}_3$ . The former is ferromagnetic below  $T_c = 27\text{ K}$ , the latter antiferromagnetic below  $T_N = 53\text{ K}$ , both exhibit orbital order.<sup>32,33,34</sup> Due to the orbital multiplicity in these  $d^1$  spin  $S = 1/2$  compounds, the upper Hubbard band consists of a series of different  $d^2$  multiplets. In  $\text{YTiO}_3$ , the lowest multiplet is identified with a peak at 2.55 eV, whereas a strongly temperature-dependent peak at 1.95 eV is attributed to an excitonic resonance. For a proper determination of  $U$  it is essential to take excitonic effects into account. We discuss the possible relevance of the kinetic energy for exciton formation in *orbitally* ordered compounds, similar to the case of a 2D antiferromagnet. Our results provide the experimental basis to disentangle the role of Coulomb and kinetic energy in 3D Mott-Hubbard insulators.

The spectral weight of the LHB-UHB excitation is expected to depend on the nearest-neighbor spin-spin correlations.<sup>35,36,37,38</sup> In a single-band model, the spectral weight vanishes in the case of ferromagnetic order due to the Pauli principle, and one expects a strong change of the spectral weight as a function of the temperature  $T$  at the magnetic ordering transition. In a multi-orbital system, the spectral weight also depends on the orbital occupation. This kind of analysis has been applied to a number of compounds with different transition-metal ions (Mn, V, Ru, Mo).<sup>4,35,36,37,38,39,40,41,42,43,44,45,46</sup> For instance in  $\text{LaMnO}_3$  and  $\text{LaSrMnO}_4$ , a quantitative description of the experimentally observed  $T$  dependence of the spectral weight has been obtained.<sup>35,38</sup> In the manganites, the  $T$  dependence is entirely ascribed to the spin-spin correlations, whereas the orbital occupation is assumed to be independent of  $T$ . This reflects the large ligand-field splitting  $\Delta_{eg}$  of roughly 1 eV of the  $e_g$  orbitals in these  $d^4$  compounds.<sup>35,38</sup> Here, we show that the  $T$  dependence of the spectral weight of  $\text{YTiO}_3$  and  $\text{SmTiO}_3$  is *not* dominated by the spin-spin correlations. This is particularly evident for  $\text{SmTiO}_3$ , where the sign of the  $T$

dependence of the spectral weight depends on the polarization. This behavior can be attributed to small changes of the orbital occupation in these  $t_{2g}$  compounds.

The paper is organized as follows. Section II addresses the experimental details. The optical conductivity of  $\text{YTiO}_3$  and  $\text{SmTiO}_3$  is reported in section III. In section III.A we first discuss the multiplet assignment and argue that the lowest peak has to be interpreted as an excitonic resonance in both compounds. A possible contribution of the kinetic energy to exciton binding in the case of antiferro-*orbital* order is proposed in section III.B. In section III.C we discuss the temperature dependence of the spectral weight and the relevance of spin-spin correlations and orbital occupation. The anisotropy of the spectral weight of the lowest multiplet in  $\text{YTiO}_3$  is addressed in section III.D. A summary and conclusions are given in section IV. The role of oxygen defects for the analysis of ellipsometric data of  $\text{YTiO}_3$  is discussed in the appendix.

## II. EXPERIMENTAL

Single crystals of  $\text{YTiO}_3$  and  $\text{SmTiO}_3$  were grown using the floating-zone technique. The crystal quality and stoichiometry were checked by x-ray diffraction, EDX, and polarization microscopy. The crystals are single phase and single domain. From magnetization measurements (SQUID, PPMS) we find that  $\text{YTiO}_3$  becomes ferromagnetic below  $T_c=27\text{ K}$  and  $\text{SmTiO}_3$  antiferromagnetic below  $T_N=53\text{ K}$ . Further details on crystal preparation and characterization can be found in Ref. 47. In  $\text{YTiO}_3$ , four-sublattice orbital order has been reported up to room temperature.<sup>32,33</sup> In both compounds an orbital-ordering transition has not been observed, i.e., they are considered to be orbitally ordered up to the melting temperature, or, in other words, the distortions arising from the orbital occupation do not break the crystal symmetry.

Generalized ellipsometric data<sup>48</sup> was obtained using a rotating-analyzer ellipsometer (Woollam VASE) equipped with a retarder between polarizer and sample. The angle of incidence was  $70^\circ$ . Immediately after polishing, the sample was kept in an UHV cryostat. The measurement background pressure of  $p < 10^{-9}$  mbar has been achieved by a bakeout at 400 K for 24 h. Window effects have been corrected using a standard Si wafer. In orthorhombic  $\text{RTiO}_3$ , only the diagonal elements  $\sigma^a$ ,  $\sigma^b$  and  $\sigma^c$  of the complex optical conductivity tensor  $\sigma(\omega) = \sigma_1 + i\sigma_2$  are finite. In  $\text{YTiO}_3$ , we have determined  $\sigma(\omega)$  from the normalized Müller matrix elements  $m_{12}^i$ ,  $m_{21}^i$ ,  $m_{33}^i$ , and  $m_{34}^i$ , where  $i = 1 - 4$  denotes different orientations of the sample, namely with *s*-polarized light parallel to the crystallographic *a* and *b* (*a*\* and *c*) axes on the *ab* (*a*\**c*) surface, where  $a^* = [110]$  within the  $Pbnm$  space group. In  $\text{SmTiO}_3$ ,  $\sigma(\omega)$  has been determined from measurements on *bc* and *ab* surfaces.

Ellipsometry is a surface sensitive technique, thus one

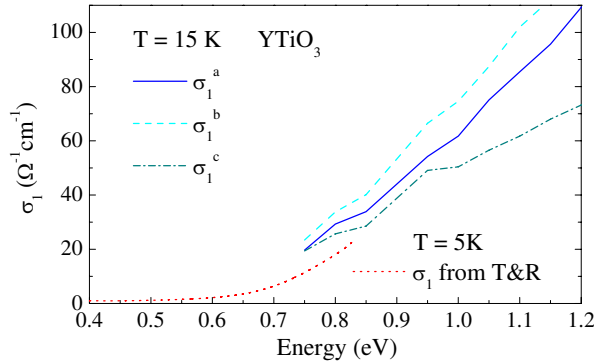


FIG. 2: (Color online) Optical conductivity of  $\text{YTiO}_3$  in the vicinity of the onset of excitations across the gap. Good agreement is observed between our ellipsometry data and results determined from the combination of transmittance and reflectance measurements.<sup>51</sup>

has to consider the possible contribution of surface contaminations or adsorbate layers. To this end we have polished and measured a sample of  $\text{YTiO}_3$  several times, both in UHV and under ambient conditions, and for different angles of incidence. The raw data show small variations which are attributed to the surface. A consistent description of all data sets for the two distinct surface orientations has been achieved by assuming a non-absorbing cover layer, where only the thickness  $d \leq 2 \text{ nm}$  of this layer has been allowed to vary for different data sets. For an extensive discussion of the data analysis, we refer to Ref. 49. The particular choice of the cover layer has a certain influence on the absolute value of  $\sigma(\omega)$ , but we emphasize that the temperature dependence is hardly affected. We also have checked carefully that the observed temperature dependence reflects the properties of  $\text{YTiO}_3$  and is not caused by changes of the cover layer, i.e., adsorbates.<sup>49</sup> We observed changes of the cover layer if we start with a base pressure of  $p = 10^{-7} \text{ mbar}$ , but not for  $p < 10^{-9} \text{ mbar}$ . In Fig. 1 we plot  $\sigma_1^a$ ,  $\sigma_1^b$ , and  $\sigma_1^c$  of  $\text{YTiO}_3$  from 0.75 to 5.8 eV at 15 K. The data are consistent with the unpolarized room-temperature data of Ref. 50 and with infrared transmittance and reflectivity results obtained in our group.<sup>51</sup> The latter revealed an onset of interband excitations at about 0.6 eV (see Fig. 2). Recently, the effect of oxygen defects at the surface of  $\text{YTiO}_3$  has been discussed.<sup>52</sup> We address this issue in the appendix.

### III. RESULTS

Undoped  $\text{YTiO}_3$  and  $\text{SmTiO}_3$  are Mott-Hubbard insulators. In the ground state there is a single electron in the  $3d$  shell at each Ti site. It is well accepted that the absorption above the gap corresponds to excitations from the LHB to the UHB, i.e., to the creation of an empty and a doubly occupied site,  $|d^1d^1\rangle \rightarrow |d^0d^2\rangle$ . The strong increase of  $\sigma_1(\omega)$  above  $\approx 4.5 \text{ eV}$  (see Fig. 1) re-

flects the onset of charge-transfer excitations from the  $\text{O}_{2p}$  band to the UHB,  $|d^1p^6\rangle \rightarrow |d^2p^5\rangle$ . The difference in spectral weight can be attributed to the Ti-O hopping  $t_{pd}$ :  $\sigma_1(\omega) \propto t_{pd}^2$  for charge-transfer excitations and  $\sigma_1(\omega) \propto t_{pd}^4/\Delta^2$  for Mott-Hubbard excitations, where  $\Delta$  denotes the charge-transfer energy.

For  $\text{YTiO}_3$ , photoemission and inverse photoemission spectroscopy<sup>47,53,54,55</sup> yield  $\Delta \cong 6 \text{ eV}$  and an on-site Coulomb interaction  $U \approx 5 \text{ eV}$ ,<sup>56</sup> where  $U$  denotes the Coulomb repulsion if both electrons occupy the *same* real orbital. In a single-band Hubbard model, the splitting between LHB and UHB is given by  $U$  (cf. inset of Fig. 1). However, for a quantitative description of  $\sigma(\omega)$  and for a reliable peak assignment one has to take all five  $3d$  orbitals into account.<sup>35,36,37,38</sup>

#### A. Multiplet assignment and Hubbard exciton

Figures 3 and 4 focus on the inter-Hubbard-band excitations of  $\text{YTiO}_3$  and  $\text{SmTiO}_3$  below 4.5 eV. In  $\text{YTiO}_3$ , three peaks are observed at 1.95 (A), 2.55 (B), and 4.15 eV (C). In  $\text{SmTiO}_3$ , we find two pronounced peaks at 1.9 and 3.7 eV. Additionally, there is a shallow shoulder at 2.5 eV, particularly noticeable for the *b* axis.

For a Mott-Hubbard insulator, one expects that a local multiplet calculation yields a reasonable assignment of the LHB-UHB excitations.<sup>35,36,37,38</sup> In terms of local multiplets, the excited  $|d^0d^2\rangle$  states can be distinguished according to the  $d^2$  sector, because  $d^0$  is an empty shell. The  $d^2$  sector is split into a series of multiplets by the electron-electron interaction, the crystal field, and the hybridization with the ligands.<sup>57</sup> We start from cubic symmetry, in which case the crystal field and the hybridization give rise to a splitting of the  $3d$  orbitals into a triply degenerate  $t_{2g}$  level and a doubly degenerate  $e_g$  level at higher energy. The splitting is denoted by 10 Dq, which roughly can be estimated as  $2 \pm 0.5 \text{ eV}$  [33,58,59,60]. The electron-electron interaction within the  $3d$  shell can be parameterized by the three Slater integrals  $F^0$ ,  $F^2$  and  $F^4$ . Values of  $F^2 = 6.75 \text{ eV}$  and  $F^4/F^2 \approx 5/8$  are characteristic for  $d^2 \text{ Ti}^{2+}$  ions in a crystal.<sup>57</sup> The only parameter that can be adapted is  $F^0$ , which drastically deviates in a solid from the ionic value due to screening effects.

For  $F^0 = 3.60 \text{ eV}$  (or  $U \approx 4.5 \text{ eV}$  [56]) the  $|d^1d^1\rangle \rightarrow |d^0d^2\rangle$  excitation energies are given in Fig. 5, focusing on the four multiplets lowest in energy: the triplet  $^3T_1$ , the singlets  $^1T_2$  and  $^1E$ , and the triplet  $^3T_2$ . For an intuitive picture we consider the strong crystal-field limit ( $10 \text{ Dq} \gg U$ ), as sketched on the right hand side of Fig. 5. In this limit, there is one electron in the  $t_{2g}$  level and one in the  $e_g$  level in the  $^3T_2$  state, whereas both electrons occupy the  $t_{2g}$  level in the three other states. It is common to consider the simplified Kanamori scheme<sup>37</sup> with the Hund on-site exchange coupling  $J_H = \frac{2.5}{49}F^2 + \frac{22.5}{441}F^4$ , resulting in  $J_H = 0.6 \pm 0.1 \text{ eV}$  for  $d^2 \text{ Ti}^{2+}$ . For  $U \cong 4 - 5 \text{ eV}$ , the Kanamori scheme predicts the lowest excitation

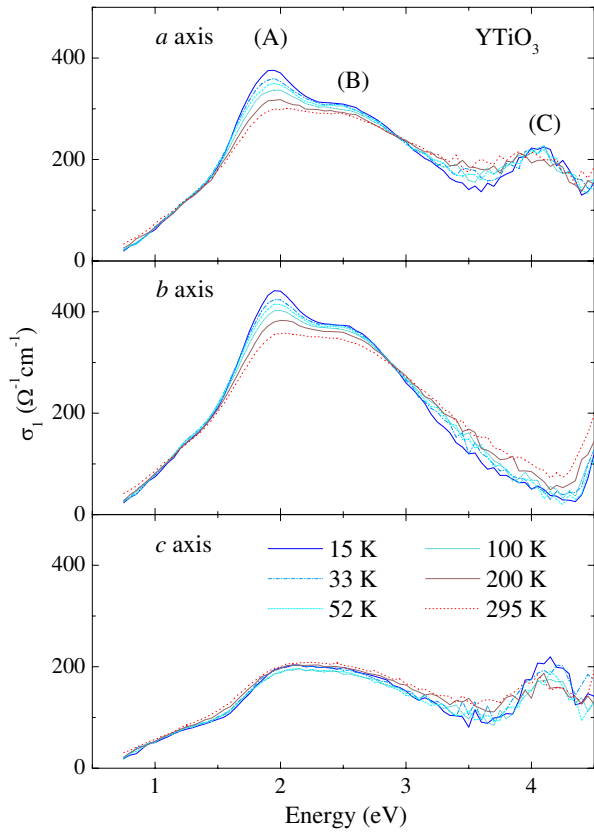


FIG. 3: (Color online) Optical conductivity of  $\text{YTiO}_3$  below the onset of charge-transfer excitations, i.e., in the range of the lowest excitations from the lower to the upper Hubbard band. Peak B is attributed to the lowest multiplet, whereas peak A is identified as an excitonic resonance. Peak C reflects the lowest excitation to an  $e_g$  orbital.

into the  $^3T_1$  triplet at  $U - 3J_H \approx 2 - 3$  eV, separated from the singlets  $^1T_2$  and  $^1E$  by  $2J_H \approx 1.2$  eV (reflecting Hund's rule) and from the  $^3T_2$  state by  $10\text{Dq} \approx 2$  eV, in qualitative agreement with the result of the rigorous calculation shown in Fig. 5.

### 1. $\text{YTiO}_3$

Figure 5 clearly shows that the  $^3T_1$  state is the lowest multiplet, more than 1.2 eV below the next multiplet for any reasonable choice of  $10\text{Dq}$ . Thus the small splitting of 0.6 eV between peaks A and B in  $\text{YTiO}_3$  cannot be identified with the difference between the  $^3T_1$  state and any other multiplet. We conclude that both peaks A and B are related to excitations into the  $^3T_1$  state. Peak C can be attributed to the  $^3T_2$  state, since only excitations into triplet states are allowed from a fully polarized ferromagnetic ground state within an electric dipole approximation. Excitations to the singlet states  $^1T_2$  and  $^1E$  require a spin flip and thus are suppressed, at least at low temperatures.

In the following, we discuss three scenarios for the

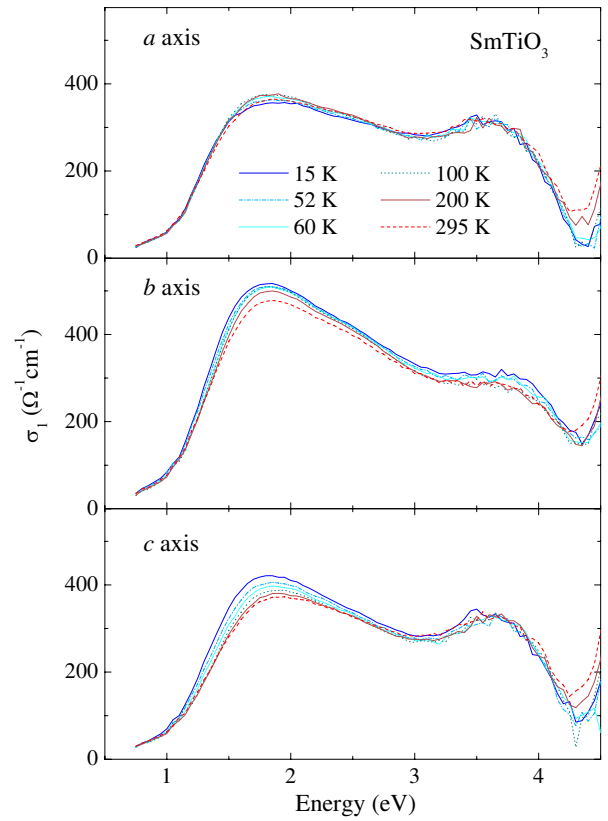


FIG. 4: (Color online) Optical conductivity of  $\text{SmTiO}_3$ .

splitting between peaks A and B: deviations from cubic symmetry, band structure effects, and an excitonic resonance. The deviation from cubic symmetry lifts the degeneracy of the  $t_{2g}$  orbitals and thereby also of the  $^3T_1$  state. The  $t_{2g}$  splitting was found to be  $\approx 0.25$  eV in infrared transmittance,<sup>51</sup> Raman scattering,<sup>61</sup> and RIXS measurements.<sup>59</sup> This is clearly too small to explain the splitting between peaks A and B.<sup>62</sup>

Now we address the possible role of band structure effects. Based on the actual crystal structure, a LDA+DMFT study of  $\text{YTiO}_3$  by Pavarini *et al.*<sup>63</sup> does not show a splitting of the lowest peak in  $\sigma_1(\omega)$ . For  $U=5$  eV and  $J_H=0.64$  eV, this peak has been predicted at 3.3 eV, and the optical gap is expected roughly at 1.5 eV. This large value of the gap suggests that a smaller value of  $U$  is more appropriate. Good agreement between the prediction for the lowest peak and the observed energy of 2.55 eV of peak B can be obtained by assuming  $U \approx 4.3$  eV. This value of  $U$  also yields a good description of the optical gap. Moreover, it corroborates the validity of our local multiplet calculation discussed above (see Fig. 5), which for  $U=4.5$  eV predicts the lowest peak at about 2.5 eV. We stress that it is unreasonable to identify peak A at 1.95 eV with the peak found in LDA+DMFT, since this would require to assume a still smaller value of  $U$ , resulting in a very small gap. Indeed the LDA+DMFT calculation finds a metallic state for  $U=3.5$  eV.<sup>63</sup>

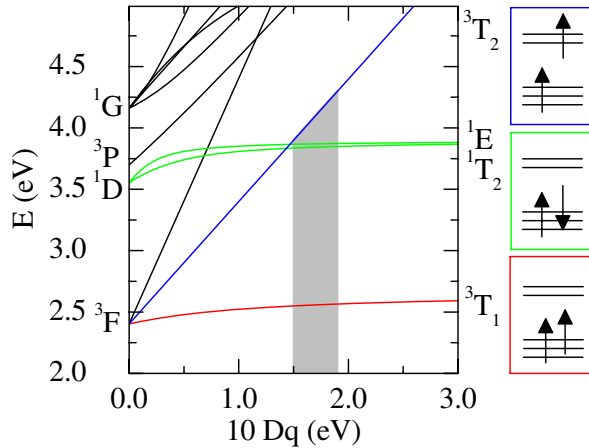


FIG. 5: (Color online) Left: Calculated energies for a  $|d^1d^1\rangle \rightarrow |d^0d^2\rangle$  excitation with different  $d^2$  final states in a cubic crystal-field.<sup>57</sup> The Slater integrals were chosen as  $F^0 = 3.60$  eV,  $F^2 = 6.75$  eV, and  $F^4 = 4.55$  eV, corresponding to  $U = 4.5$  eV [56] and  $J_H \approx 0.6$  eV. For  $10 Dq = 0$  the ionic multiplet structure is obtained. For  $10 Dq \approx 1.5 - 1.9$  eV (grey area) the energy of 4.15 eV for peak C is well described by excitations into the  $^3T_2$  state. Right: sketch of the orbital occupation in the strong crystal-field limit for the  $^3T_1$  triplet (red), the  $^1T_2$  and  $^1E$  singlets (green), and the  $^3T_2$  triplet (blue).

Also the LDA+DMFT study by Craco *et al.*<sup>64</sup> for the ferromagnetic phase of  $Y\text{TiO}_3$  finds a single peak in  $\sigma_1(\omega)$ . Based on the parameter values of  $U = 4.75$  eV and  $J_H = 1.0$  eV, Craco *et al.* attribute this peak to peak A observed at 1.95 eV in our data. However,  $J_H$  is not expected to deviate strongly from the ionic value of  $J_H = 0.6 \pm 0.1$  eV discussed above. The lowest peak in  $\sigma_1(\omega)$  is located at about  $U - 3J_H$ , thus the choice of  $J_H = 1.0$  eV strongly underestimates the peak frequency. We emphasize that both LDA+DMFT studies<sup>63,64</sup> find a *single* peak in  $\sigma_1(\omega)$ . Both studies investigate an effective Hamiltonian for the  $t_{2g}$  sector, i.e., excitations to the higher-lying  $^3T_2$  multiplet (peak C) are not considered.

Experimental data neither support a splitting due to band-structure effects. In photoemission (PES) data of  $Y\text{TiO}_3$  the LHB is a single peak  $\approx 1.3$  eV below the Fermi level.<sup>47,53,55,65</sup> In inverse PES on  $Y_{1-x}\text{Ca}_x\text{TiO}_3$  ( $x = 0$  [65] and  $0.4 - 0.8$  [55]) the UHB can be identified with the lowest peak or shoulder  $\approx 1.5 - 2$  eV above the Fermi level. Both PES and inverse PES agree with the LDA+DMFT result<sup>63</sup> for  $U = 4 - 5$  eV. Finally,  $U \approx 5.3$  eV has been derived from  $2p$  core-level PES [54] (see [56] for the comparison of parameters derived by different methods).

Altogether, both theoretical and experimental results support our interpretation that the splitting of 0.6 eV between peaks A and B does not result from the band structure and that peak B at 2.55 eV is the dominant excitation.

In contrast to (inverse) PES, the optical conductivity reflects particle-hole excitations and thus is sensi-

tive to interactions between the particle in the UHB (i.e. a double occupancy) and the hole in the LHB. These interactions are also neglected in the LDA+DMFT calculations<sup>63,64</sup> of  $\sigma_1(\omega)$ . We therefore identify peak B at 2.55 eV as a particle-hole excitation in which the particle and the hole are well separated, whereas peak A at 1.95 eV is interpreted as an excitonic resonance, where the particle and the hole remain close to each other. Note that peak A does not lie below the gap, i.e., it is not a truly bound exciton, but a resonance within the continuum. As discussed above, a Hubbard exciton may arise due to the attractive Coulomb interaction between the particle and the hole. The nearest-neighbor electron-electron repulsion  $V$  of the extended Hubbard model<sup>6,7,8,9,10,11,12,13,14</sup> is equivalent to a particle-hole attraction  $-V$  [66]. We are not aware of an accurate experimental value of  $V$  for the titanates, but it is reasonable to assume  $V \leq 1$  eV. For the 1D charge-transfer insulator  $\text{SrCuO}_2$ , a value of  $V \approx 0.6$  eV has been derived from the comparison of the line shape of the excitonic resonance in  $\sigma_1(\omega)$  with predictions from dynamical density-matrix renormalization group calculations for an effective extended Hubbard model.<sup>13</sup> More detailed theoretical studies of the extended Hubbard model in 3D are required to decide whether the nearest-neighbor Coulomb interaction is sufficient to explain the splitting of 0.6 eV observed between peaks A and B.

## 2. $\text{SmTiO}_3$

The magnetic ground state of  $RT\text{O}_3$  changes from ferromagnetic to antiferromagnetic as a function of the size of the  $R$  ions.<sup>71,72</sup> This change is accompanied by a crossover of both the character of the distortions of the oxygen octahedra and of the orbital-ordering pattern.<sup>34,71,72,73</sup> The optical conductivity of the antiferromagnet  $\text{SmTiO}_3$  is given in Fig. 4, focusing on the range of the Mott-Hubbard bands below the onset of charge-transfer excitations at about 4.5 eV. At 300 K we observe two pronounced peaks at 1.9 and 3.7 eV and a shallow shoulder at 2.5 eV, most evident for the  $b$  axis. The multiplet structure discussed above for  $Y\text{TiO}_3$  also applies to  $\text{SmTiO}_3$ . In particular, one does not expect appreciable changes of the Slater integrals, i.e., of the electronic parameters  $U$  and  $J_H$ . This is corroborated by the LDA+DMFT calculations by Pavarini *et al.*,<sup>63</sup> which predict the same peak frequency for  $\sigma_1(\omega)$  in  $Y\text{TiO}_3$  and in the antiferromagnet  $\text{LaTiO}_3$ . Therefore we identify the shoulder at 2.5 eV in  $\text{SmTiO}_3$  with peak B at 2.55 eV in  $Y\text{TiO}_3$ , whereas the asymmetric peak at 1.8 eV is attributed to an excitonic resonance (see below), equivalent to peak A in  $Y\text{TiO}_3$ .

In contrast to the peak energies, the band width or equivalently the hopping matrix elements are expected to change significantly, resulting from the different Ti-O-Ti bond angles. A larger band width of  $\text{SmTiO}_3$  agrees with the observation from transmittance measurements<sup>51</sup> that

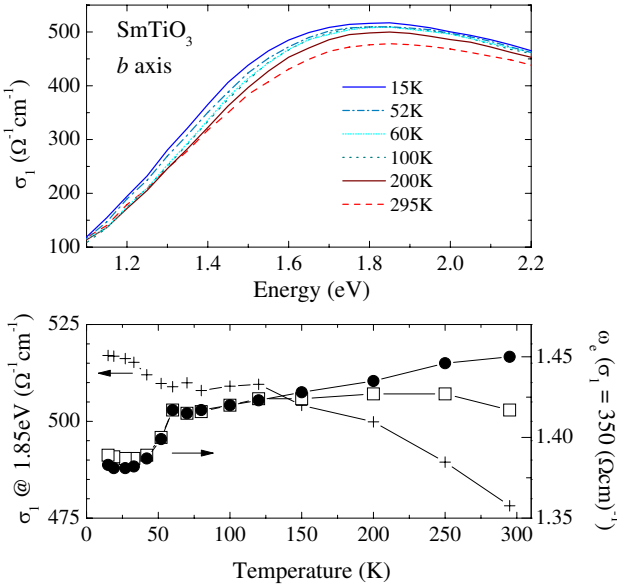


FIG. 6: (Color online) Top: Leading edge of the optical conductivity  $\sigma_1^b(\omega)$  of SmTiO<sub>3</sub>. Bottom: Temperature dependence of  $\sigma_1^b(\omega = 1.85 \text{ eV})$  (crosses, left axis) and of the leading edge  $\omega_e$ , which we define by  $\sigma_1^b(\omega_e) = 350 \text{ (Ωcm)}^{-1}$  (full symbols, right axis). Open symbols show  $\tilde{\omega}_e$  corrected for the change of the spectral weight, i.e.,  $\sigma_1^b(\tilde{\omega}_e) = c \cdot 350 \text{ (Ωcm)}^{-1}$  with  $c = \sigma_1^b(1.85 \text{ eV}, T) / \sigma_1^b(1.85 \text{ eV}, 60 \text{ K})$ .

the gap in SmTiO<sub>3</sub> is about 0.2 eV lower than in YTiO<sub>3</sub>. Additionally, an increase of the hopping amplitudes gives rise to an increase of the spectral weight. This is further enhanced by the change of the orbital ground state.<sup>71,72</sup> Experimentally, we find an increase of  $N_{\text{eff}}$  from YTiO<sub>3</sub> to SmTiO<sub>3</sub> of roughly 25%, 50%, and 100% for the  $a$ ,  $b$ , and  $c$  axes, respectively.

As discussed above for YTiO<sub>3</sub>, an interpretation of the peak at 1.9 eV in terms of the lowest multiplet is hard to reconcile with the LDA+DMFT result,<sup>63</sup> unless excitonic effects are considered. An exciton interpretation is supported by the temperature dependence of the peak frequency observed for the  $b$  and  $c$  axes, showing an anomalous softening with decreasing temperature and an anomaly at  $T_N$ . For the  $b$  axis we demonstrate this softening in Fig. 6. We focus on the frequency  $\omega_e$  of the leading edge, which we define as  $\sigma_1^b(\omega_e) = 350 \text{ (Ωcm)}^{-1}$ . This has the advantage that  $\omega_e$  and also its temperature dependence can be determined more accurately than the peak frequency itself. The disadvantage is that a softening of  $\omega_e$  in principle can be caused not only by a softening of the peak frequency, but also by an increase of either the spectral weight or the line width, and by a change of the line shape. We find a jump-like decrease of  $\omega_e$  at  $T_N$ , see lower panel of Fig. 6. This cannot be attributed to an increased line width, since the thermal contribution to the line width is expected to decrease with decreasing temperature. Moreover, for *spin-carrying* particles one expects that the band width is reduced upon entering the AF ordered state, thus the

gap is expected to *harden*. For an estimate of the  $T$  dependence of the spectral weight we consider the value of  $\sigma_1(\omega)$  at the peak frequency. We find an increase of  $\sigma_1^b(\omega = 1.85 \text{ eV})$  upon cooling below  $T_N$  (see crosses in bottom panel of Fig. 6), indicating an increase of the spectral weight. We use this  $T$  dependence of the absolute value to determine a corrected frequency of the leading edge,  $\tilde{\omega}_e$ , defined as  $\sigma_1^b(\tilde{\omega}_e) = c \cdot 350 \text{ (Ωcm)}^{-1}$  with  $c = \sigma_1^b(1.85 \text{ eV}, T) / \sigma_1^b(1.85 \text{ eV}, 60 \text{ K})$  (open symbols in Fig. 6). This shows that the shift of  $\omega_e$  is not due to the change of the spectral weight, it is caused mainly by a softening of the peak frequency or a change of the line shape. Both can be rationalized by the attractive interactions responsible for exciton formation, pulling the spectral weight to lower frequencies.

The excitonic binding due to the kinetic energy is enhanced in the AF ordered state, as discussed for 2D compounds in the introduction. Remarkably, the peak frequency of 1.95 eV is independent of temperature in the ferromagnet YTiO<sub>3</sub>. It is an interesting question whether this difference between the two compounds arises from a change of the screening of nearest-neighbor Coulomb interactions, of the magnetic ground state, or of the orbital ordering pattern. A decisive identification of the driving force for exciton formation requires further theoretical investigations of the extended multi-orbital Hubbard model in 3D.

The peak at 3.7 eV coincides with the minimum of  $\sigma_1(\omega)$  observed in YTiO<sub>3</sub>. This peak can be attributed to the lowest singlet multiplet (<sup>1</sup>T<sub>2</sub> and <sup>1</sup>E in cubic symmetry). Due to the spin selection rule, the excitation to the singlet state is suppressed in ferromagnetic YTiO<sub>3</sub>, but it is allowed in antiferromagnetic SmTiO<sub>3</sub>. This feature is expected at about  $2J_H \approx 1.2 - 1.3 \text{ eV}$  above the lowest triplet peak, providing further support for the assignment of peak B at 2.5 eV and the excitonic character of the peaks at 1.8 eV in SmTiO<sub>3</sub> and 1.95 eV in YTiO<sub>3</sub>.

## B. Hubbard exciton and orbital order

For a 2D Mott-Hubbard insulator with AF exchange  $J$  on a square lattice, exciton formation is governed by the *kinetic* energy.<sup>18,19,20,21,22</sup> The motion of a single particle is hindered by the interaction of its spin with the AF background. This can be described in terms of a spin polaron. Hopping of the bare particle on the energy scale  $t$  results in a trace of misaligned spins. Coherent motion of the dressed polaronic quasiparticle requires the emission of magnons, i.e., the bare band width  $\sim t$  is reduced to the polaronic band width  $\sim J$ , which corresponds to an increase of kinetic energy. In this case, the kinetic energy is lowered by the formation of *spinless* excitons, which recover a larger band width.

This mechanism may contribute to exciton binding in antiferromagnetic SmTiO<sub>3</sub>, but not in ferromagnetic YTiO<sub>3</sub>. It is promising to investigate whether a similar mechanism is at work in the case of antiferro-*orbital*

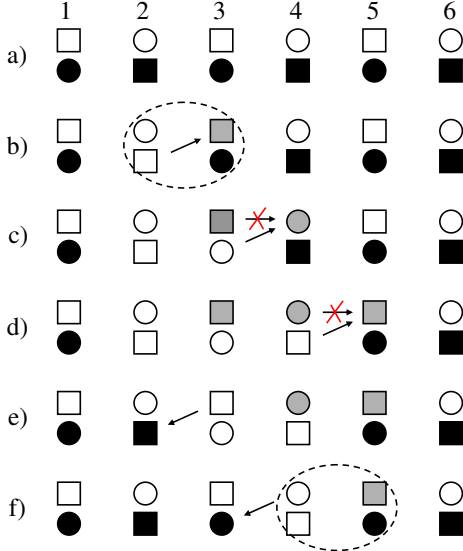


FIG. 7: Sketch of the suggested formation and propagation of a Hubbard exciton (dashed line). We consider two types of orbitals (circles and squares, e.g.,  $d_{xy}$  and  $d_{xz}$ ) per site, where hopping is zero between orbitals of different type (crossed out arrows). Full (open) symbols denote occupied (empty) orbitals. (a) Ground state with antiferro-orbital order. (b) Creation of a hole and a double occupancy on sites 2 and 3, respectively. (c)–(f) Propagation of the double occupancy, the hole, or of an exciton (see main text for more details).

order. For illustration and simplicity, we consider a 1D model with two orbitals per site, e.g.,  $d_{xy}$  and  $d_{xz}$  for a chain running along the  $x$  direction. In Fig. 7, the two types of orbitals are denoted by circles and squares, respectively. Hopping between neighboring sites is allowed only between orbitals of the same type; it is zero between orbitals of different type. Black and grey symbols in Fig. 7 refer to occupied orbitals, whereas empty symbols denote empty orbitals. The ground state in Fig. 7a exhibits antiferro-orbital order, i.e.,  $xy$  (circles) and  $xz$  orbitals (squares) are occupied in an alternate fashion. The empty orbitals are at higher energies due to, e.g., the ligand-field splitting. An excitation from the LHB to the UHB, i.e.,  $|d^1d^1\rangle \rightarrow |d^0d^2\rangle$ , is illustrated in Fig. 7b. Site 2 is empty, and site 3 is doubly occupied. The motion of the double occupancy to sites 4 and 5 is depicted in Figs. 7c and d, respectively. The central point is that this motion leaves a trace of orbitally excited states, i.e., on sites 3 and 4 the energetically unfavorable orbitals are occupied (grey symbols). This results from the restriction that hopping is only allowed within the same type of orbital. As discussed above for the case of spins, coherent motion of the quasi-particle requires the emission of orbital excitations, in our example the de-excitation of sites 3 and 4. Therefore, the band width is reduced from the bare band width  $\sim t$  to the energy scale of the orbital excitations, corresponding to an increase of kinetic energy. However, if the hole accompanies the double occupancy forming an exciton (dashed line), the motion of

the hole heals out the trace of excited orbitals, see Fig. 7e and f. Therefore, the motion of the exciton is not hindered by the antiferro-orbital order, and the exciton can hop on a larger energy scale than the hole or the double occupancy individually. Thus exciton formation here is equivalent to a *gain of kinetic energy*.

More detailed knowledge on the value of the nearest-neighbor Coulomb interaction  $V$  and its relationship to the binding energy in 3D Mott-Hubbard insulators is required to decide whether this mechanism is realized in  $\text{YTiO}_3$ . The orbital ordering pattern in  $\text{YTiO}_3$  is more complex than simple antiferro-orbital order,<sup>32,33</sup> and hopping between orbitals of different type is not exactly zero. Still Fig. 7 may be relevant for the  $ab$  plane, since hopping from the lowest orbital on one site (a “circle” in Fig. 7) to the lowest orbital on a neighboring site (equivalent to a “square”) is 2–3 times smaller than hopping to the excited states.<sup>60,63</sup>

### C. Temperature dependence of the spectral weight: spin and orbital selection rules

The spectral weight is determined by the spin and orbital selection rules.<sup>4,35,36,37,38,39,40,41,42,43,44,45,46</sup> Therefore, the  $T$  dependence of the spectral weight is expected to reflect changes of the spin-spin correlations and/or of the orbital occupation. By considering the nearest-neighbor spin-spin correlations, the absolute value of the spectral weight has been calculated for instance for  $\text{LaMnO}_3$  [4,35,36] and  $\text{LaSrMnO}_4$  [38]. These calculations yield a convincing description of the experimental results, the maximum difference is less than a factor of 2. For a 3D magnet one expects that the spin-spin correlations are small above the ordering temperature. In fact, the change of the spectral weight above  $T_N$  is small in the 3D antiferromagnet  $\text{LaMnO}_3$ .<sup>35</sup> In contrast, the 2D antiferromagnet  $\text{LaSrMnO}_4$  with a Néel temperature of  $T_N = 130$  K, exhibits a significant  $T$  dependence of the spectral weight up to 300 K, which can be attributed to enhanced quantum fluctuations in 2D.<sup>38</sup>

For the lowest excited triplet state ( ${}^3T_1$  in cubic notation) of orbitally ordered  $\text{YTiO}_3$ , Oles *et al.*<sup>36</sup> predicted a change of 25% of the spectral weight between the paramagnetic and the ferromagnetic state in the  $ab$  and  $c$  directions. This can be understood by the evolution of the nearest-neighbor spin-spin correlation function  $\langle \mathbf{S}_i \cdot \mathbf{S}_j + 3/4 \rangle$ , which equals 1 in the ferromagnetic state and  $3/4$  in the paramagnetic state, i.e., a redistribution of 25%.

We analyze the integrated spectral weight in terms of the effective carrier concentration  $N_{\text{eff}}$ ,

$$N_{\text{eff}} = \frac{2mV_0}{\pi e^2} \int_{\omega_{c1}}^{\omega_{c2}} \sigma_1(\omega) d\omega \quad (1)$$

where  $\omega_{c1}$  and  $\omega_{c2}$  denote the frequency range of interest,  $m$  is the free electron mass,  $e$  the elementary charge, and  $1/V_0$  the density of Ti ions. For  $V_0$  we use the value

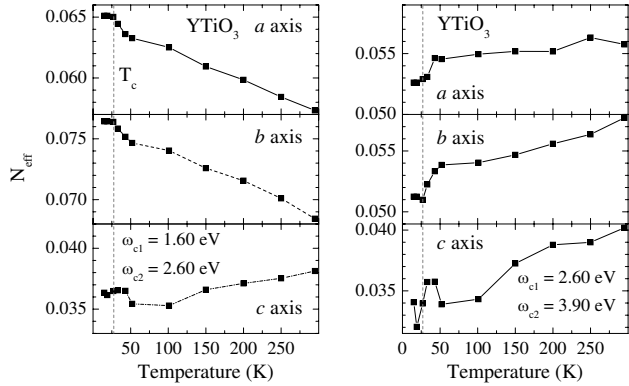


FIG. 8: Temperature dependence of the effective carrier concentration  $N_{\text{eff}}$  (see Eq. 1) of  $\text{YTiO}_3$  for  $\omega_{c1} = 1.6 \text{ eV}$  and  $\omega_{c2} = 2.6 \text{ eV}$  (left) and for  $\omega_{c1} = 2.6 \text{ eV}$  and  $\omega_{c2} = 3.9 \text{ eV}$  (right).

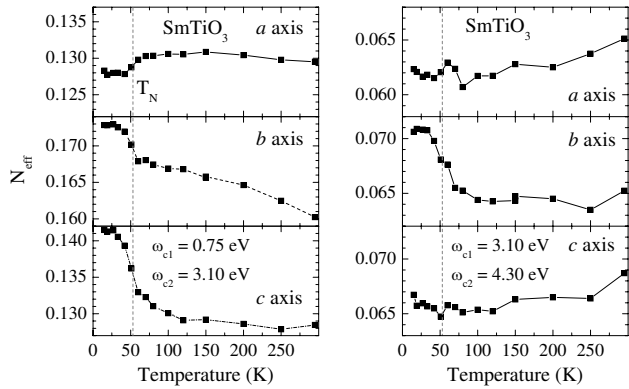


FIG. 9: Temperature dependence of the effective carrier concentration  $N_{\text{eff}}$  (see Eq. 1) of  $\text{SmTiO}_3$  for  $\omega_{c1} = 0.75 \text{ eV}$  and  $\omega_{c2} = 3.1 \text{ eV}$  (left) and for  $\omega_{c1} = 3.1 \text{ eV}$  and  $\omega_{c2} = 4.3 \text{ eV}$  (right).

observed at 290 K, which differs from the 2 K value by less than 1%.<sup>34</sup> The  $T$  dependence of  $N_{\text{eff}}$  is given in Fig. 8 for  $\text{YTiO}_3$  and in Fig. 9 for  $\text{SmTiO}_3$ . In  $\text{YTiO}_3$ , the spectral weight increases between 1.6 and 2.6 eV (left panel of Fig. 8) in the  $a$  and  $b$  directions upon cooling down from room temperature. We find an anomaly in the vicinity of  $T_c$ , i.e., an additional increase of spectral weight with decreasing temperature. This additional increase starts at about  $1.5 - 2 T_c$  and amounts to less than 5% below 50 K, much smaller than predicted. At the same time, one finds an anomalous decrease of spectral weight with decreasing temperature between 2.6 and 3.9 eV, again in  $a$  and  $b$ . Moreover, the spin selection rule cannot explain that the spectral weight in this 3D ferromagnet shows a strong  $T$  dependence up to 300 K  $> 10 T_c$ .

In  $\text{SmTiO}_3$ , we also find pronounced anomalies in the vicinity of the magnetic ordering temperature,  $T_N = 53 \text{ K}$ . The strongest change of  $N_{\text{eff}}$  of up to 10% is observed in the  $c$  axis, significantly larger than in  $\text{YTiO}_3$ . In  $\text{SmTiO}_3$ , the *sign* of the change at  $T_N$  depends on the polarization (see left panel of Fig. 9), which certainly

cannot be attributed to the spin selection rule in a  $G$ -type antiferromagnet. In comparison to the excellent agreement found between experiment and theory in the manganites,<sup>35,38</sup> this failure appears as a puzzle.

Alternatively, we consider the orbital selection rule. In the manganites, the orbital occupation has been assumed to be independent of  $T$  due to the large  $e_g$  splitting of roughly 1 eV.<sup>35,38</sup> In both  $\text{YTiO}_3$  and  $\text{SmTiO}_3$ , the  $t_{2g}$  splitting is only  $\approx 0.25 \text{ eV}$  [51,59,61], opening the possibility for small changes of the orbital occupation as a function of  $T$ . A change of the orbital occupation affects the effective Ti-Ti hopping amplitude  $t$ , with  $N_{\text{eff}} \propto t^2 \propto t_{pd}^4 / \Delta^2$ . An increase of the occupation of the planar  $xy$  orbital may for instance give rise to an increase of the spectral weight within the  $xy$  plane accompanied by a decrease of spectral weight along  $z$ . Thus a change of the orbital occupation at  $T_N$  can very well account for the observed polarization dependence. Based on a detailed analysis of the crystal structure, thermal expansion and magnetostriction of  $RT\text{O}_3$ , Komarek *et al.*<sup>34</sup> conclude that magnetism affects the crystal structure, which in turn drives a change of the orbital occupation. Remarkably, the shape of the oxygen octahedra changes significantly as a function of temperature, whereas the variation of the tilt and rotation angles is small.<sup>34</sup> Both the lattice distortions and the orbital occupation adapt in order to enhance the gain of energy within the spin system. The effect is most pronounced at the magnetic ordering temperature, but extends also to higher temperatures, in agreement with our data. Moreover, Komarek *et al.*<sup>34</sup> pointed out that the change of the orbital occupation is significantly stronger in  $\text{SmTiO}_3$  than in  $\text{YTiO}_3$ , again in agreement with our results. The occurrence of pronounced effects in  $\text{SmTiO}_3$  is attributed to the fact that  $\text{SmTiO}_3$  is close to the crossover from antiferromagnetic to ferromagnetic order.<sup>34</sup> In the optical data, the effect of the orbital selection rule possibly overrules that of the spin selection rule, which appears as a failure of the latter.

Note that the change of the lattice constants at  $T_N$  can only account for a change of  $N_{\text{eff}}$  of the order of 1%. This estimate is based on the Harrison rules<sup>74</sup> for the hopping amplitudes. We emphasize that binding phenomena such as the formation of excitons or resonances in general are very sensitive to temperature. With decreasing temperature, the attractive interactions responsible for the exciton formation pull down the spectral weight to lower energies, in agreement with the change of the line shape observed in  $\text{YTiO}_3$  (see Fig. 3) and the shift of the absorption edge of  $\text{SmTiO}_3$  discussed above (see Fig. 6).

#### D. Anisotropy

In order to understand the anisotropy observed in  $\text{YTiO}_3$  between the  $ab$  plane and the  $c$  direction, we address the matrix elements for the optical excitation  $|d^1d^1\rangle \rightarrow |d^0d^2\rangle$ . Our Hamiltonian includes the crys-

tal field, the on-site Coulomb correlations of the  $d^2$  configurations, and the hopping between the two Ti sites (for details, see Ref. 60). We find realistic values of the exchange coupling constants for the different directions as well as an orbital ground state which is in excellent agreement with x-ray, neutron and other theoretical results.<sup>32,33,51,63,67</sup> From the effective Ti-Ti hopping matrices  $t^{ab}$  and  $t^c$  one can estimate the anisotropy of the spectral weight from

$$\frac{N_{\text{eff}}^{ab}}{N_{\text{eff}}^c} = \frac{N_{\text{eff}}^a + N_{\text{eff}}^b}{2N_{\text{eff}}^c} = \sum_{j=2,3} \frac{(t_{1j}^{ab})^2 + (t_{j1}^{ab})^2}{(t_{1j}^c)^2 + (t_{j1}^c)^2}, \quad (2)$$

where  $t_{ij}$  denotes the effective hopping matrix element between the  $t_{2g}$  orbitals  $i$  and  $j$  on adjacent sites. We obtain  $N_{\text{eff}}^{ab}/N_{\text{eff}}^c \approx 5.1$ . Using the hopping matrices published by other groups, we find a value of 1.1 [68] or 3.5 [63]. In the next step the optical conductivity has been calculated using the Kubo formula. We assume a fully polarized ferromagnetic ground state. We address only excitations into the lowest triplet state with a  $t_{2g}^2$  configuration, because here the point-charge approximation gives reliable results. We predict  $N_{\text{eff}}^{ab}/N_{\text{eff}}^c \approx 4.5$ . The small difference to the value of 5.1 derived from the simplified approach considered in Eq. 2 arises because here the energies of the excited states and the Ti-Ti distance are taken into account. For  $\omega_{c1} = 1.6$  eV and  $\omega_{c2} = 2.6$  eV (see Eq. 1), we experimentally find  $N_{\text{eff}}^{ab}/N_{\text{eff}}^c \approx 2$  (see Fig. 8), within the range predicted by the different theoretical approaches.

#### IV. SUMMARY AND CONCLUSIONS

In summary, we report on optical excitations from the lower to the upper Hubbard band in the ferromagnet  $\text{YTiO}_3$  and in the antiferromagnet  $\text{SmTiO}_3$ . At 15 K we find peaks in the optical conductivity  $\sigma_1(\omega)$  at 1.95, 2.55, and 4.15 eV in  $\text{YTiO}_3$  and at 1.8 and 3.7 eV in  $\text{SmTiO}_3$ , which also exhibits a shallow shoulder at 2.5 eV. For these Mott-Hubbard insulators, a local multiplet scenario is expected to yield a reasonable peak assignment, as reported for the manganites.<sup>35,38</sup> For  $U \approx 4.5$  eV and  $J_H = 0.6 \pm 0.1$  eV, our local multiplet calculation offers a quantitative description of the peak positions at 2.5, 3.7 and 4.15 eV. The peak at about 2.5 eV is attributed to excitations into the lowest  $d^2$  multiplet ( ${}^3T_1$  in cubic symmetry) with an energy of roughly  $U - 3J_H$  [62]. The peak at 3.7 eV corresponds to the lowest  $d^2$  singlet states, and the peak at 4.15 eV is attributed to the lowest state with a  $t_{2g}^1 e_g^1$  configuration. This assignment is in agreement with photoemission and LDA+DMFT results. The peaks at 1.95 eV in  $\text{YTiO}_3$  and 1.8 eV in  $\text{SmTiO}_3$  are interpreted in terms of an excitonic resonance, thereby explaining their low energy.

The temperature dependence of the spectral weight disagrees with predictions based on the spin selection rule. In  $\text{YTiO}_3$  the observed temperature dependence

is much smaller than predicted, whereas in  $\text{SmTiO}_3$  even the sign of the temperature dependence disagrees for certain polarization directions, a puzzling result. However, a small change of the orbital occupation at the magnetic ordering temperature<sup>34</sup> can account for the polarization dependence and also explains the larger temperature dependence found for  $\text{SmTiO}_3$ . In contrast to the manganites, such a change of the orbital occupation is feasible in  $\text{RTiO}_3$  because the  $t_{2g}$  splitting amounts to only 0.25 eV. Furthermore, the increase of spectral weight at low frequencies with decreasing temperature is in agreement with an exciton scenario, since binding phenomena are expected to exhibit a strong temperature dependence. An increased binding at low temperatures pulls down spectral weight to lower frequencies and also explains the anomalous softening of the leading absorption edge observed in  $\text{SmTiO}_3$ .

The importance of excitonic effects for the description of  $\sigma(\omega)$  is well established for low-dimensional correlated insulators. The attractive interaction responsible for exciton formation arises from a gain of either Coulomb or kinetic energy. We have pointed out that exciton formation may lower the kinetic energy in an orbitally ordered state. Our results call for further theoretical studies of exciton formation in the extended multi-orbital Hubbard model in 3D. A quantitative description of this binding phenomenon is essential for a consistent explanation of optical and photoemission data and will provide important information on electronic correlations in Hubbard systems.

#### Acknowledgement

We thank I. Simons and M. Cwik for technical support, and T. Wagner, D.I. Khomskii, G.S. Uhrig, E. Pavarini, O.K. Andersen, N. Blümer, G. Khaliullin, T. Möller, and S.V. Streltsov for fruitful discussions. This work is supported by the DFG in SFB 608.

#### Appendix: Role of oxygen defects

Recently, Kovaleva *et al.*<sup>52</sup> studied  $\text{YTiO}_3$  by ellipsometry and reported on complications which they attribute to oxygen defects arising from polar surfaces. They observed peaks in  $\sigma_1(\omega)$  at 1.95, 2.9, and 3.7 eV. The overall temperature dependence observed in Ref. 52 is very weak, showing a crossover at 100 K, but no anomaly at  $T_c$  within the experimental accuracy. In the frequency range studied by us, the main effects of oxygen defects were identified as (i) a shift of the fundamental absorption edge to lower frequencies, (ii) an absorption band at about 0.8 eV, (iii) the absence of a pronounced minimum at 4.5 eV, and (iv) a shift of the onset of charge-transfer excitations to lower frequencies. These shifts have been attributed to localized states at the edge of the electronic bands. This sensitivity of the fundamental absorption

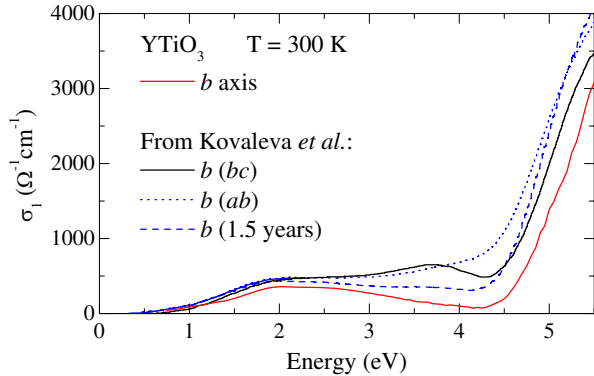


FIG. 10: (Color online) Comparison of the optical conductivity for the *b* axis of  $\text{YTiO}_3$  with spectra reported by Kovaleva *et al.*,<sup>52</sup> which were determined from either the *ab* or the *bc* surface of a freshly polished sample, or from the *ab* surface of a sample measured after 1.5 years.

edge to doping away from the half-filled Mott insulator has been studied in  $\text{Y}_{1-x}\text{Ca}_x\text{TiO}_3$  [69,70]. In Fig. 10 we compare our data with the results of Ref. 52. Our data show both the largest fundamental absorption edge and the largest onset frequency for charge-transfer excitations, in combination with a pronounced minimum at 4.5 eV. We find good agreement with the spectrum of  $\sigma_1(\omega)$  below the fundamental gap determined in our group by transmittance and reflectance measurements on thin single crystals<sup>51</sup> (see Fig. 2). The transmittance clearly reveals bulk properties. These data show no defect-induced absorption below the gap, the single weak feature observed at about 0.3 eV has been undoubtedly identified as a phonon-activated orbital excitation.<sup>51,59,61</sup> Finally, we find clear anomalies in the vicinity of the magnetic ordering temperatures, both in  $\text{YTiO}_3$  and in  $\text{SmTiO}_3$  (see Figs. 8 and 9). The combination of all these observations provides strong evidence that we have observed the intrinsic properties of  $\text{YTiO}_3$ .

- <sup>1</sup> G. Kotliar and D. Vollhardt, Physics Today **3**, 53 (2004).
- <sup>2</sup> M. Imada, A. Fujimori, and Y. Tokura, Rev. Mod. Phys. **70**, 1039 (1998).
- <sup>3</sup> Y. Tokura and N. Nagaosa, Science **288**, 462 (2000).
- <sup>4</sup> G. Khaliullin, Prog. Theor. Phys. Suppl. **160**, 155 (2005).
- <sup>5</sup> D.I. Khomskii, Physica Scripta **72**, CC8 (2005).
- <sup>6</sup> J. van den Brink, M.B.J. Meinders, J. Lorenzana, R. Eder, and G. A. Sawatzky, Phys. Rev. Lett. **75**, 4658 (1995).
- <sup>7</sup> F.B. Gallagher and S. Mazumdar, Phys. Rev. B **56**, 15025 (1997).
- <sup>8</sup> R. Neudert, M. Knupfer, M.S. Golden, J. Fink, W. Stephan, K. Penc, N. Motoyama, H. Eisaki, and S. Uchida, Phys. Rev. Lett. **81**, 657 (1998).
- <sup>9</sup> F.H.L. Essler, F. Gebhard, and E. Jeckelmann, Phys. Rev. B **64**, 125119 (2001).
- <sup>10</sup> A. Hübsch, J. Richter, C. Waidacher, K.W. Becker, and W. von der Linden, Phys. Rev. B **63**, 205103 (2001).
- <sup>11</sup> E. Jeckelmann, Phys. Rev. B **67**, 075106 (2003).
- <sup>12</sup> A.S. Moskvin, J. Málek, M. Knupfer, R. Neudert, J. Fink, R. Hayn, S.-L. Drechsler, N. Motoyama, H. Eisaki, and S. Uchida, Phys. Rev. Letters **91**, 037001 (2003).
- <sup>13</sup> Y.-J. Kim, J.P. Hill, H. Benthien, F.H.L. Essler, E. Jeckelmann, H.S. Choi, T.W. Noh, N. Motoyama, K.M. Kojima, S. Uchida, D. Casa, and T. Gog, Phys. Rev. Lett. **92**, 137402 (2004).
- <sup>14</sup> H. Matsueda, T. Tohyama, and S. Maekawa, Phys. Rev. B **71**, 153106 (2005).
- <sup>15</sup> M. Ono, K. Miura, A. Maeda, H. Matsuzaki, H. Kishida, Y. Taguchi, Y. Tokura, M. Yamashita, and H. Okamoto, Phys. Rev. B **70**, 085101 (2004).
- <sup>16</sup> M. Ono, H. Kishida, and H. Okamoto, Phys. Rev. Lett. **95**, 087401 (2005).
- <sup>17</sup> H. Kishida, H. Matsuzaki, H. Okamoto, T. Manabe, M. Yamashita, Y. Taguchi, and Y. Tokura, Nature **405**, 929 (2000).
- <sup>18</sup> D.G. Clarke, Phys. Rev. B **48**, 7520 (1993).
- <sup>19</sup> Y.Y. Wang, F.C. Zhang, V.P. Dravid, K.K. Ng, M.V. Klein, S.E. Schnatterly, and L.L. Miller, Phys. Rev. Lett. **77**, 1809 (1996).
- <sup>20</sup> F.C. Zhang and K.K. Ng, Phys. Rev. B **58**, 13520 (1998).
- <sup>21</sup> P. Wrobel and R. Eder, Phys. Rev. B **66**, 035111 (2002).
- <sup>22</sup> R.O. Kuzian, R. Hayn, and A.F. Barabanov, Phys. Rev. B **68**, 195106 (2003).
- <sup>23</sup> M.E. Símon, A.A. Aligia, C.D. Batista, E.R. Gagliano, and F. Lema, Phys. Rev. B **54**, R3780 (1996).
- <sup>24</sup> E. Hanamura, N.T. Dan, and Y. Tanabe, Phys. Rev. B **62**, 7033 (2000); J. Phys.: Condens. Matter **12**, L345 (2000).
- <sup>25</sup> A.S. Moskvin, R. Neudert, M. Knupfer, J. Fink, and R. Hayn, Phys. Rev. B **65**, 180512(R) (2002).
- <sup>26</sup> H. Gomi, A. Takahashi, T. Ueda, H. Itoh, and M. Aihara, Phys. Rev. B **71**, 045129 (2005).
- <sup>27</sup> H. Itoh, A. Takahashi, and M. Aihara, Phys. Rev. B **73**, 075110 (2006).
- <sup>28</sup> E. Collart, A. Shukla, J.-P. Rueff, P. Leininger, H. Ishii, I. Jarrige, Y.Q. Cai, S.-W. Cheong, and G. Dhaleen, Phys. Rev. Lett. **96**, 157004 (2006).
- <sup>29</sup> D.S. Ellis, J.P. Hill, S. Wakimoto, R.J. Birgeneau, D. Casa, T. Gog, and Y.-J. Kim, Phys. Rev. B **77**, 060501(R) (2008).
- <sup>30</sup> J.E. Hirsch Phys. Rev. Lett. **59**, 228 (1987); Science **295**, 2226 (2002).
- <sup>31</sup> H.J.A. Molegraaf, C. Presura, D. van der Marel, P.H. Kes, and M. Li, Science **295**, 2239 (2002).
- <sup>32</sup> J. Akimitsu, H. Ichikawa, N. Eguchi, T. Miyano, M. Nishi, and K. Kakurai, J. Phys. Soc. Jpn. **70**, 3475 (2001).
- <sup>33</sup> F. Iga, M. Tsubota, M. Sawada, H.B. Huang, S. Kura, M. Takemura, K. Yaji, M. Nagira, A. Kimura, T. Jo, T. Takabatake, H. Namatame, and M. Taniguchi, Phys. Rev. Lett. **93**, 257207 (2004).
- <sup>34</sup> A.C. Komarek, H. Roth, M. Cwik, W.-D. Stein, J. Baier, M. Kriener, F. Bourée, T. Lorenz, and M. Braden, Phys. Rev. B **75**, 224402 (2007).
- <sup>35</sup> N.N. Kovaleva, A.V. Boris, C. Bernhard, A. Kulakov, A. Pimenov, A.M. Balbashov, G. Khaliullin, and B. Keimer, Phys. Rev. Lett. **93**, 147204 (2004).
- <sup>36</sup> A.M. Oles, G. Khaliullin, P. Horsch, and L.F. Feiner, Phys.

Rev. B **72**, 214431 (2005).

<sup>37</sup> J. S. Lee, M. W. Kim, and T. W. Noh, New J. Phys. **7**, 147 (2005).

<sup>38</sup> A. Gössling, M.W. Haverkort, M. Benomar, Hua Wu, D. Senff, T. Möller, M. Braden, J.A. Mydosh, and M. Grüninger, Phys. Rev. B **77**, 035109 (2008).

<sup>39</sup> K. H. Ahn and A. J. Millis, Phys. Rev. B **61**, 13545 (2000).

<sup>40</sup> K. Tobe, T. Kimura, Y. Okimoto, and Y. Tokura, Phys. Rev. B **64**, 184421 (2001).

<sup>41</sup> J. S. Lee, Y. S. Lee, T. W. Noh, S.-J. Oh, J. Yu, S. Nakatsuji, H. Fukazawa, and Y. Maeno, Phys. Rev. Lett. **89**, 257402 (2002).

<sup>42</sup> M. W. Kim, Y. S. Lee, T. W. Noh, J. Yu, and Y. Moritomo, Phys. Rev. Lett. **92**, 027202 (2004).

<sup>43</sup> R. Rauer, M. Rübhausen, and K. Dörr, Phys. Rev. B **73**, 092402 (2006).

<sup>44</sup> S. Miyasaka, Y. Okimoto, and Y. Tokura, J. Phys. Soc. Jpn. **71**, 2086 (2002).

<sup>45</sup> A. A. Tsvetkov, F. P. Mena, P. H. M. van Loosdrecht, D. van der Marel, Y. Ren, A. A. Nugroho, A. A. Menovsky, I. S. Elfimov, and G. A. Sawatzky, Phys. Rev. B **69**, 075110 (2004).

<sup>46</sup> G. Khaliullin, P. Horsch, and A. M. Oleś, Phys. Rev. B **70**, 195103 (2004).

<sup>47</sup> H. Roth, PhD thesis, University of Cologne (2008).

<sup>48</sup> M. Schubert, Phys. Rev. B **53**, 4265 (1996).

<sup>49</sup> A. Gössling, Ph.D. thesis, University of Cologne (2007); <http://nbn-resolving.de/urn:nbn:de:hbz:38-21379>

<sup>50</sup> T. Arima, Y. Tokura, and J.B. Torrance, Phys. Rev. B **48**, 17006 (1993).

<sup>51</sup> R. Rückamp, E. Benckiser, M.W. Haverkort, H. Roth, T. Lorenz, A. Freimuth, L. Jongen, A. Möller, G. Meyer, P. Reutler, B. Büchner, A. Revcolevschi, S.-W. Cheong, C. Sekar, G. Krabbes, and M. Grüninger, New J. Phys. **7**, 144 (2005).

<sup>52</sup> N.N. Kovaleva, A.V. Boris, P. Yordanov, A. Maljuk, E. Brücher, J. Strempfer, M. Konuma, I. Zegkinoglou, C. Bernhard, A.M. Stoneham, and B. Keimer, Phys. Rev. B **76**, 155125 (2007).

<sup>53</sup> A. Fujimori, I. Hase, H. Namatame, Y. Fujishima, Y. Tokura, H. Eisaki, S. Uchida, K. Takegahara, and F.M.F. de Groot, Phys. Rev. Lett. **69**, 1796 (1992).

<sup>54</sup> A.E. Bocquet, T. Mizokawa, K. Morikawa, A. Fujimori, S.R. Barman, K. Maiti, D.D. Sarma, Y. Tokura, and M. Onoda, Phys. Rev. B **53**, 1161 (1996).

<sup>55</sup> K. Morikawa, T. Mizokawa, A. Fujimori, Y. Taguchi, and Y. Tokura, Phys. Rev. B **54**, 8446 (1996).

<sup>56</sup> For a comparison of different results one needs to distinguish between  $U = F^0 + \frac{4}{49}F^2 + \frac{36}{441}F^4$  (both electrons occupy the *same* real orbital) and  $U_{av} = F^0 - \frac{14}{441}(F^2 + F^4)$  (averaged over all multiplets) with the Slater integrals  $F^0$ ,  $F^2$ , and  $F^4$ . The value of  $U_{av} \cong 4$  eV reported in Ref. 54 corresponds to  $U \approx 5.3$  eV. However, this value is based on a  $\text{TiO}_6$  configuration-interaction cluster model including covalency. Due to screening effects by  $\text{O}_{2p}$  orbitals, the effective value of  $U$  is somewhat smaller, in good agreement with  $U=4.5$  eV chosen in Fig. 5.

<sup>57</sup> S. Sugano, Y. Tanabe, and H. Kamimura, *Multiplets of Transition-Metal Ions in Crystals* (Academic Press, New York, 1970).

<sup>58</sup> T. Higuchi, T. Tsukamoto, M. Watanabe, M.M. Grush, T.A. Callcott, R.C. Perera, D.L. Ederer, Y. Tokura, Y. Harada, Y. Tezuka, and S. Shin, Phys. Rev. B **60**, 7711 (1999).

<sup>59</sup> C. Ulrich, G. Ghiringhelli, A. Piazzalunga, L. Braicovich, N.B. Brookes, H. Roth, T. Lorenz, and B. Keimer, Phys. Rev. B **77**, 113102 (2008).

<sup>60</sup> R. Schmitz, O. Entin-Wohlman, A. Aharony, and E. Müller-Hartmann, Annalen der Physik **16**, 425 (2007); Annalen der Physik **14**, 626 (2005).

<sup>61</sup> C. Ulrich, A. Gössling, M. Grüninger, M. Guennou, H. Roth, M. Cwik, T. Lorenz, G. Khaliullin, and B. Keimer, Phys. Rev. Lett. **97**, 157401 (2006).

<sup>62</sup> The  $t_{2g}$  splitting  $\Delta_{t_{2g}}$  is relevant for a precise determination of  $U$ , since the lowest non-excitonic excitation (peak B) is expected at about  $U - 3J_H + \Delta_{t_{2g}}$ .

<sup>63</sup> E. Pavarini, A. Yamasaki, J. Nuss, and O.K. Andersen, New J. Phys. **7**, 188 (2005).

<sup>64</sup> L. Craco, S. Leoni, M.S. Laad, and H. Rosner, Phys. Rev. B **76**, 115128 (2007).

<sup>65</sup> M. Arita, H. Sato, M. Higashi, K. Yoshikawa, K. Shimada, M. Nakatake, Y. Ueda, H. Namatame, M. Taniguchi, M. Tsubota, F. Iga, and T. Takabatake, Phys. Rev. B **75**, 205124 (2007).

<sup>66</sup> In Mott-Hubbard insulators, the particle and the hole may reside on the *same* site, albeit with different spin or orbital quantum numbers. Such a very strongly bound “exciton” corresponds to a magnon or an orbiton, excitations within the spin or orbital channel. There is no doubly occupied site and one does not have to pay the energy  $U$ , in contrast to the excitations discussed here.

<sup>67</sup> S.V. Streltsov, A.S. Mylnikova, A.O. Shorikov, Z.V. Pchelkina, D.I. Khomskii, and V.I. Anisimov, Phys. Rev. B **71**, 245114 (2005).

<sup>68</sup> I.V. Solovyev, Phys. Rev. B **73**, 155117 (2006).

<sup>69</sup> Y. Okimoto, T. Katsufuji, Y. Okada, T. Arima, and Y. Tokura, Phys. Rev. B **51**, 9581 (1995).

<sup>70</sup> Y. Taguchi, Y. Tokura, T. Arima, and F. Inaba, Phys. Rev. B **48**, 511 (1993).

<sup>71</sup> M. Mochizuki and M. Imada, New J. Phys. **6**, 154 (2004).

<sup>72</sup> M. Mochizuki and M. Imada, J. Phys. Soc. Jpn. **73**, 1833 (2004).

<sup>73</sup> M. Kubota, H. Nakao, Y. Murakami, Y. Taguchi, M. Iwama, and Y. Tokura, Phys. Rev. B **70**, 245125 (2004).

<sup>74</sup> W.A. Harrison, *Elementary electronic structure* (World Scientific, 1999).